OBSERVATIONS OF LOW-LEVEL MESOCYCLOGENESIS USING A NEW TRAJECTORY MAPPING TECHNIQUE

Daniel Betten[1], Michael I. Biggerstaff[1], Gordon Carrie[1]

[1] *University of Oklahoma, Norman, Oklahoma, USA, Daniel.P.Betten-1@ou.edu*

(Dated: 26 August 2011)

I. INTRODUCTION

On 29 May 2004 during the Thunderstorm and Electrification Experiment (TELEX; MacGorman et al. 2008), a high precipitation thunderstorm initiated along a dryline in western Oklahoma in the United States of America and produced over a dozen tornadoes as it propagated across Oklahoma. The storm was observed for nearly 2 hours by two mobile C-band Doppler radars (Biggerstaff et al. 2005) that were deployed along a ~42 km baseline oriented nearly parallel to the storm motion. High temporal resolution of the Doppler data permitted calculation of individual air trajectories, which are illustrated here using a novel trajectory mapping technique. This study focuses on the period from 0018 ~ 0048 UTC.

II. METHODS

Software from the National Center for Atmospheric Research (NCAR) was used to edit, interpolate and synthesize the radar data. Backward trajectories were calculated using a 4th order Runge-Kutta scheme and a linear interpolation in time with a variable storm motion derived from a least-squares minimization of the low-level mesocyclone position.

To visualize the evolution of airflow through the storm, trajectories were initialized every 250 m, with an inner area every 50 m, over a 25 km x 25 km region encompassing the mesocyclone. Characteristics of the flow along each trajectory were then plotted spatially at 30 s intervals to elucidate differences in source region and vorticity evolution for air within and near the mesocyclone. This procedure allowed for analysis of trajectory attributes in the same reference frame as the dual-Doppler syntheses. Contour plots were made from variables at a specific time, the maximum or minimum along the trajectory, and integration of a variable along the trajectory.

II. RESULTS AND DISCUSSION

The trajectory mapping technique helps to visualize the time integrated advection and deformation processes affecting the airflow. Characteristics of the flow, on scales smaller than the analyzed Euclidian dual-Doppler analysis appear to be well retrieved. For example, the dual-Doppler analysis of 1.2 km vertical motion at 0029 UTC shows a divided mesocyclone structure with a strong downdraft to the south of the mesocyclone center (Fig. 1a). The downdraft extended to the surface but decreased in magnitude. A map of the source region of air at 500 m altitude based on a 10-minute backward trajectory starting at 0029 UTC (Fig. 1b) reveals that most of the downdraft region consisted of air that had originated at low levels that had been carried first in an updraft before being entrained into the downdraft. Only a small area of the mesocyclone consisted of air that was brought from significantly higher altitudes where evaporational cooling might have taken place. Hence, smaller scale characteristics of the air in the mesocyclone are easier to discern in the trajectory map framework since it better illustrates the integrated motion of individual air parcels than the instantaneous dual-Doppler synthesis.

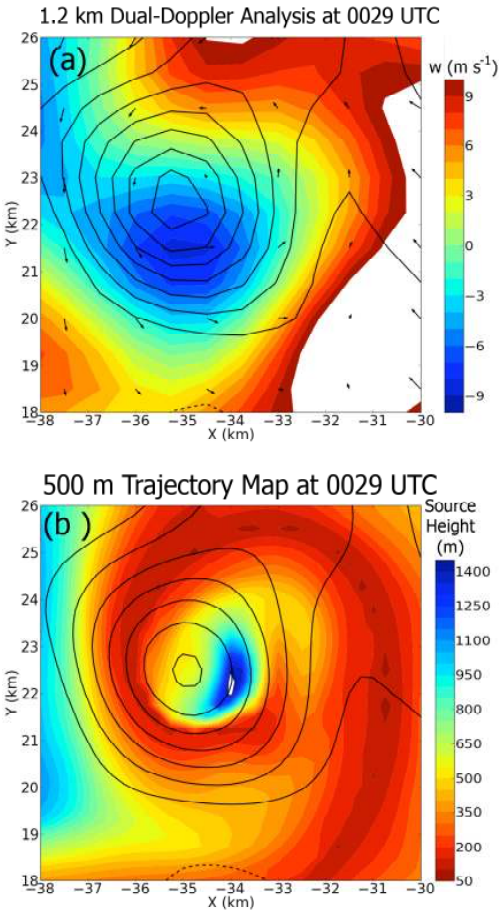

Figure 1. (a) Horizontal cross-section of vertical motion (color), storm-relative flow (arrows) and vertical vorticity (contoured every $5X10^{-3}$ s^{-1}) over the mesocyclone. (b) Horizontal map at 500 m altitude showing source height of air from 10-min backward trajectory initiated at 500 m altitude at 0029 UTC with contours of vertical vorticity overlaid as in (a).

Evolution of the air trajectories revealed air from different source regions flowed into the hook echo. Periodic downdrafts within close proximity to the low level mesocyclone and surges of inflow air around the circulation were observed to occur until the low level mesocyclone began occluding during the later analyses. The flow regime surrounding the low level mesocyclone was found to be highly sensitive to the location and intensity of the "rainy downdraft" (Brandes 1981) and the occlusion downdraft (Klemp and Rotunno 1983). Two strong surges in the Rear Flank Downdraft (RFD) occurred at 0029 and 0045 UTC (Fig. 2). Both surges coincided with an intensification of the low level mesocyclone. However, only the second surge lead to an occlusion.

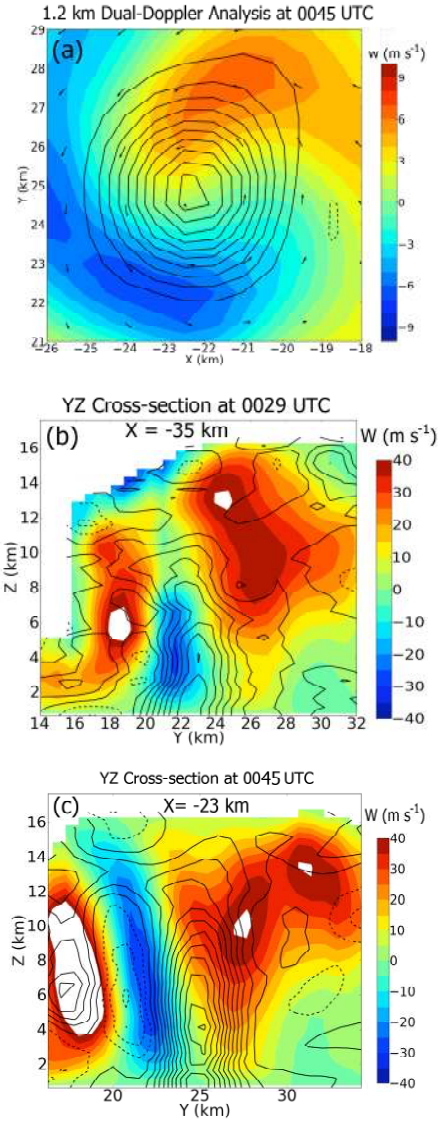

Figure 2. Horizontal (a) and vertical cross-sections (b, c) of vertical velocity (color scale) and vertical vorticity (contoured every $5X10^{-3}$ s^{-1} with negative values dashed) from the dual-Doppler analyses at the times and locations noted.

The first RFD formed close to the circulation center at low levels and was found within the circulation throughout its depth (Figs. 1a and 2b). The downdraft axis was on or just inside the radius of maximum tangential winds. After 0029, the circulation broadened and weakened temporarily, similar to observations of axial downdrafts by Brandes (1978) and Wakimoto and Lui (1998). However, the circulation reintensified and deepened after the circulation became colocated with a deep updraft. The next RFD surge at 0045 UTC developed on the outside of the core flow of the circulation (Figs. 2a, c) and coincided with a weakening of the vertical gradient of vertical vorticity, suggesting that the second RFD surge was less driven by vorticity dynamics than the first surge.

Due to the proximity of the first downdraft to the circulation center, air passing through the downdraft was advected inward and the source altitude of air on the eastern side of the circulation decreased (not shown), coinciding with weakening and broadening of the circulation. As air descended in the downdraft, it also disrupted the horizontal entrainment of air into the circulation on the south and western sides of the circulation.

One method to visualize the pattern of flow is through plots of the generation of streamwise horizontal vorticity by gradients in precipitation loading (PLSTRM; Wakimoto and Cai 2000). Air that passed along the edge of the forward flank acquired high PLSTRM while inflow air from the environment retained low values of PLSTRM. In the first RFD surge, air from the forward flank (high values of PLSTRM) was diverted to the south of the circulation while the inflow air was diverted to the north (Fig. 3a). The result was that the high PLSTRM air was concentrated on the periphery of the circulation and not able to penetrate into the mesocyclone.

The later RFD surge started as an intensifying rainy downdraft just west of the circulation. The rainy downdraft air was entrained around the periphery of the circulation, coinciding with intensification of the low level mesocyclone. While the circulation intensified, an occlusion downdraft formed on the south side of the circulation on the outside of the radius of maximum tangential wind. The location of this downdraft relative to the circulation core created a much different advection pattern than the first downdraft surge.

Downdraft air was concentrated towards the gust front and the periphery of the circulation. The inflow and forward flank air was entrained into the circulation at a smaller radius than the downdraft air. The resulting advection and deformation yielded an inner vortex with a core filled with a spiral pattern of low-level inflow and forward flank air (Fig. 3b), though unresolved mixing would likely lead to less sharp gradients. Surrounding this core was a band of forward flank air that experienced positive tilting of horizontal vorticity in the rainy downdraft. That air, which originated from slightly higher altitudes than the core air, may have acted like a buffer between the inner vortex and the less buoyant downdraft air that increased in areal coverage with time during the occlusion stage.

The differences in the location and intensity of the RFD surges also affected the pattern of vertical vorticity derived from the value at the beginning of the trajectory (in time) modified by the integrated tilting and stretching along the trajectory (Fig. 4). Initially, the trajectory map of vertical vorticity showed an annular pattern with a maximum on the periphery of the larger scale circulation (Fig. 4a). As divergence from the first RFD surge advected air from higher levels into the circulation, the region of inflow air was reduced, leaving only a small maximum in derived vertical vorticity in the circulation center (Fig. 4b).

This vorticity structure is similar to that found in high resolution numerical simulations (Klemp and Rotunno 1983,

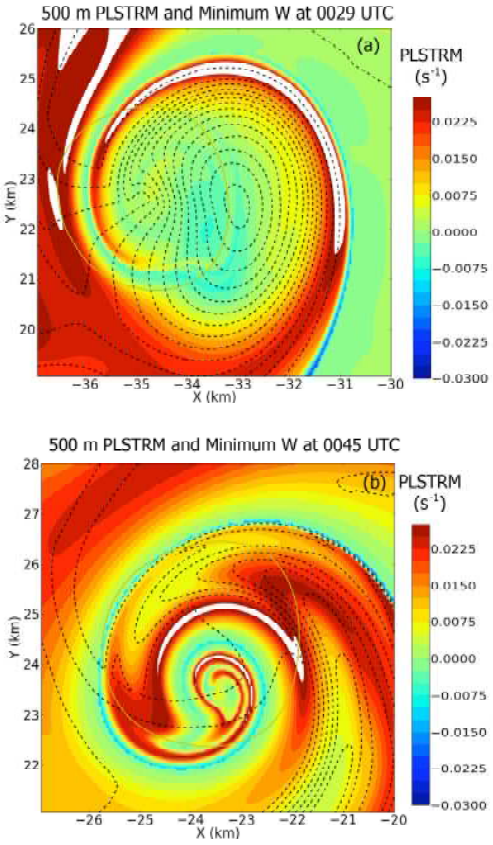

Figure 3. Horizontal maps at 500 m of time integrated generation of streamwise horizontal vorticity by gradients in precipitation loading (PLSTRM, color scale) with contours of maximum downdraft (every 0.5 m s^{-1}) along the 10-min backward trajectory initiated at (a) 0029 UTC and (b) 0045 UTC.

Wicker and Wilhelmson 1995, Gaudet and Cotton 2006) that show a pronounced transition from an annular to a concentrated circular pattern of vorticity around the time of tornadogenesis.

Later, as the mesocyclone became embedded in an updraft, the vorticity pattern became more circular (Fig. 4c). The second strong RFD surge was located farther from the core of the mesocyclone than the first and did not produce as much banding in derived vertical vorticity.

IV. SUMMARY

A new trajectory mapping technique allowed fine-scale diagnosis of complex airflow patterns through a mesocyclone in the same frame of reference as the dual-Doppler derived wind fields but with much greater fidelity. The tornadic supercell examined here had two strong RFD surges that affected the distribution of low-level vorticity and the distribution of forward-flank and inflow air around the core of the mesocyclone. The location of the RFD relative to the center of the circulation led to fundamentally different advection and deformation patterns that may have aided tornadogenesis and occlusion of the mesocyclone.

V. ACKNOWLEDGMENTS

This work was supported by the National Science Foundation grants ATM-0619715 and ATM-0802717.

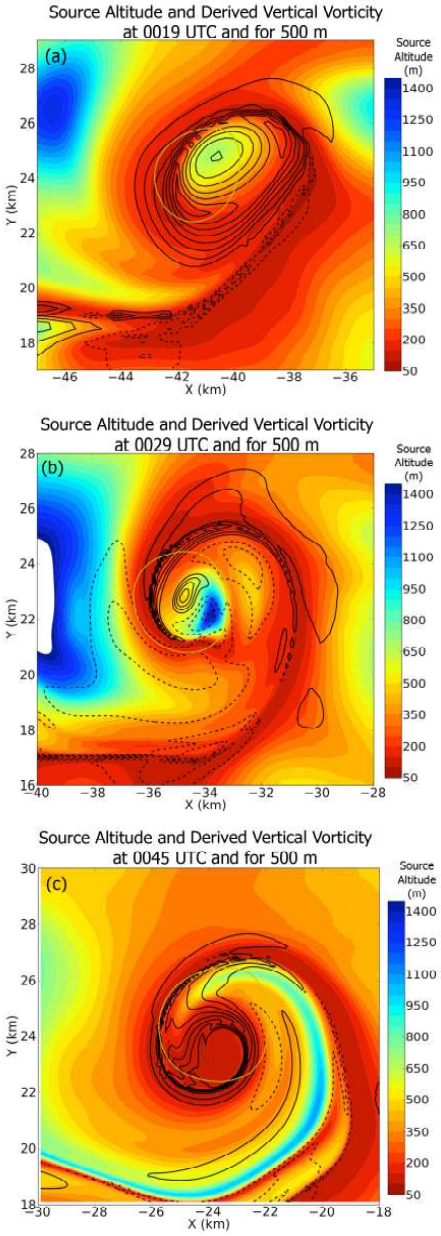

Figure 4. Horizontal maps of the source altitude of air from 10-minute backward trajectories initiated at 500m and (a) 0019 UTC, (b) 0029 UTC and (c) 0045 UTC with derived vertical vorticity contoured every 5X10^{-3} s^{-1}.

VI. REFERENCES

Biggerstaff, M., and Coauthors 2005: The Shared Mobile Atmospheric Research and Teaching Radar: A Collaboration to Enhance Research and Teaching. *Bull. Amer. Meteor. Soc.*, **86**, 1263–1274.

Brandes E., 1978: Mesocyclone evolution and tornadogenesis: Some observations. *Mon. Wea. Rev.*, **106,** 995–1011.

——, 1981: Finestructure of the Del City–Edmond tornadic mesocirculation. *Mon. Wea. Rev.,***109,** 635–647.

Gaudet B., Cotton W., 2006: Low-Level Mesocyclonic Concentration by Nonaxisymmetric Transport. Part I: Supercell and Mesocyclone Evolution. *J. Atmos. Sci.*, **63**, 1113–1133.

Klemp J., Rotunno R., 1983: A study of the tornadic region within a supercell thunderstorm. *J. Atmos. Sci.*, **40**, 359–377.

MacGorman D., and Coauthors, 2008: TELEX The Thunderstorm Electrification and Lightning Experiment. *Bull. Amer. Meteor. Soc.*, **89**, 997–1013.

Wakimoto R., and Cai H., 2000: Analysis of a nontornadic storm during VORTEX 95. *Mon. Wea. Rev.*, **128,** 565–592.

Wicker L., and Wilhelmson R., 1995: Simulation and analysis of tornado development and decay within a three-dimensional supercell thunderstorm. *J. Atmos. Sci.*, **52,** 2675–2703.